INTERNATIONAL JOURNAL OF RESEARCH IN PHARMACY AND CHEMISTRY

Available online at www.ijrpc.com

Research Article

SYNTHESIS AND CHARACTERIZATION OF INORGANIC POLYMER NANO – COMPOSITES FROM ACRYLONITRILE AND ALUMINUM CHLORIDE AND HEXACHLORO PALATINATE (IV)

Nada M. Abbass, Ahmed Qasim and Safaa Zamel*

Department of Chemistry, College of Science, University of Baghdad, Iraq.

ABSTRACT

The polymer nanocomposites (a) Al_2O_3 Fe_2O_4 (b) $PtO_2Fe_2O_4$ were synthesized by ferric chloride target metal salts and acrylonitrile aqueous solution 2:1 molar ratio with stirring. FTIR, x-ray diffraction (XRD), atomic force microcopy (AFM), thermogravimetric analysis (TG of DTG) and differential scanning calorimetry (DSC) were employed to character the resultant nanocomposites. The results of XRD and AFM indicated that the nanocomposites were a hybrid of the polymer and the metal oxides nanoparticles which were distributed uniformly in general. The FTIR spectra of oxides (a and b) looked in the rang 428-635 cm^{-1} which shows the formation of a single phase spinal structure having two sub lattices, tetrahedral and octahedral sites. Two peaks appear in the range of 1134-1137 cm^{-1} are due to C-O stretching by anhydride group in the metal oxides,confirms the acrylonitrile formed as polymer with spinal oxide. The (TG of DTG) analysis gave an indication of the thermal dissociation nature of the inorganic nancomposites at high temperatures. DSC characterization of nanocomposites materials appeared the effect of fillers on the crystallization behavior of the pure acrylonitrile. The corrosion resistance in saline water (3.5 % NaCl) at 293 K were studied.

Keywords: composites , acrylonitrile, aluminum chloride, corrosion, XRD.

INTRODUCTION

The aim of the preparation of the "nanocomposite" is to gain the synergic effect of the polymer and the inorganic compound. Nanocomposites have strange structure, a phase separated structure, with a nanoscale interface between the polymer matrix and the inorganic compound (nanophase separated structure)[1.]Polymer nanocomposite is a polymer or a "co-Polymer" having dispersed in its Nano particles[2.] The coordination polymers are also important for synthesizing the inorganic polymer nanocomposites[3,] which display prominent mechanical characteristics, heat resistance and chemical resistance compared to the heat or classic filled resins[4.] Polymer composites containing ferrites are increasing replacing the classical ceramic magnetic materials because of their mouldability and reduction in cast[5,6,7.] The synthesis of polymer nanocomposites is a complete aspect of polymer Nano technology by introduce the Nano metric inorganic compounds[8.] Tania Ribeiro and J.Farinha reported that the hybrid organic/inorganic materials combine the solidity and high thermal stability of the inorganic material with flexibility, ductility and process ability of the organic polymers[9.]

MATERIALS AND METHODS

MATERIALS AND MEASUREMENT

The chemical reagents, $FeCl_3.6H_2O$, $AlCl_3.6H_2O$, $H_2PtCl_6.6H_2O$, $(NH_4)_2$ S_2O_8, acrylonitrile and NaOH were used as obtained. Without further purifications, all reagents were used which are analytical grade.

Preparation of standard solution

A aqueous solution of acrylonitrile(acrylonitrile: water: 3:1) and 5% ammonium per sulphate solution were prepared for experiment. The standard solution was prepared by dissolving stoichiometric amounts of the metal salts in distilled water. The sodium hydroxide solution was standardized against a solution of oxalic acid as a primary standard solution and it was titrated as dibasic acid. 25 ml of oxalic acid and 8 drops of phenolphthalein was titrated with the NaOH solution, often neutralized of all the acid, a more stable pink color was appeared, stirred often addition of the last drop of NaOH.

Synthesis of complexes

The complexes were prepared according to a method described by B.P.Singh[10] .Scheme (1) illustrates the preparation of the polymer nanocomposites.

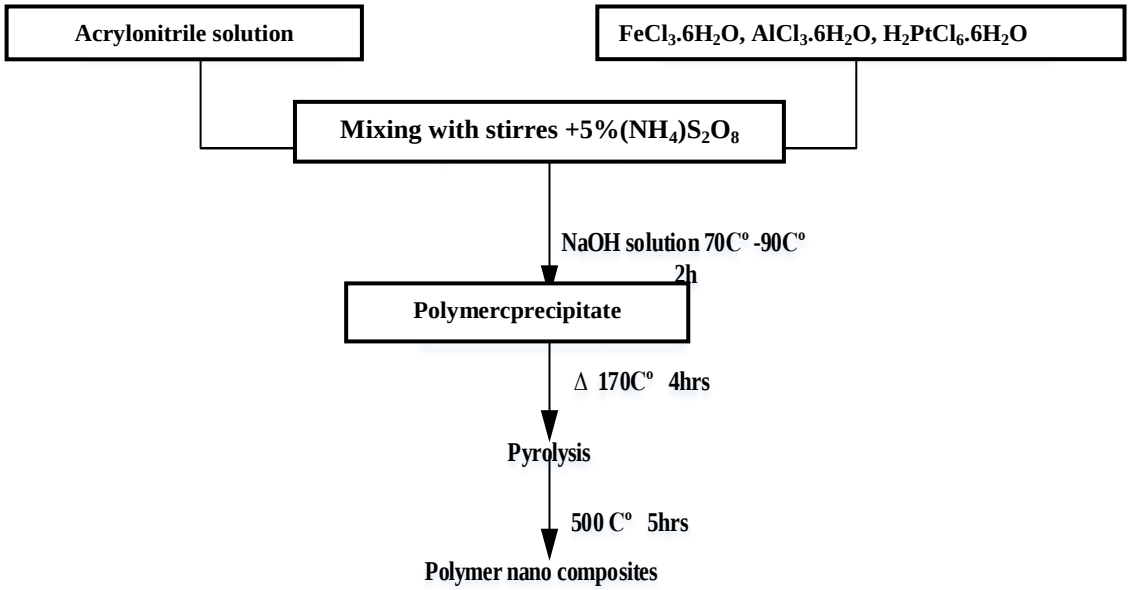

Scheme 1.Prepartion rote of polymer Nano composite

Ferric chloride solution (10 ml, 0.1 N) were added to 10 ml of acrylonitrile solution (acrylonitrile: water:7:3) with stirring. At 70-90 °C, 5%$(NH_4)_2S_2O_8$ (5ml) added to the above solution for two hours. The solution were dried to yield the poly acrylonitrile which were dried at 90-100°C ever night and were heated at 170 °C about 4 hours to obtained the amorphous nature of salt. The last salts were heated at 500 °C for five hours in air, quietly cooled and collected.

FI-IR spectroscopy

The FI-IR (fig. 1 and 2) of compounds a, b display the $\upsilon\ c-c$ and υ c – o stretching were certain due to the aspect of peaks at 1137 – 1134 cm^{-1}, helped the anhydride group of acrylonitrile ready in compounds (a +b) as polymeric from. The bands in the region 465-619 cm^{-1}certain the formation of single phase spinal structures.[11]

Table 1: FT.IR spectra of compounds

Compounds	Wave numbers of absorption band υ (cm^{-1})			
	$\upsilon\ (c-o)$	$\upsilon(\ c-c)$	Single phase spinal structure	
Al Fe_2O_4	1137	1454	υ_4 611	υ_5 465
Pt Fe_2O_4	1134	1458	619	457

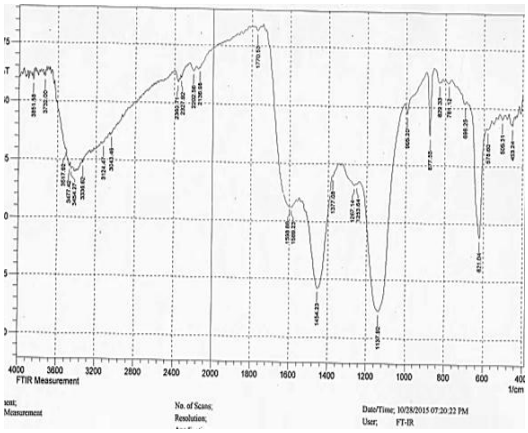

Fig. 1: FT-IR spectrum of compound (a)

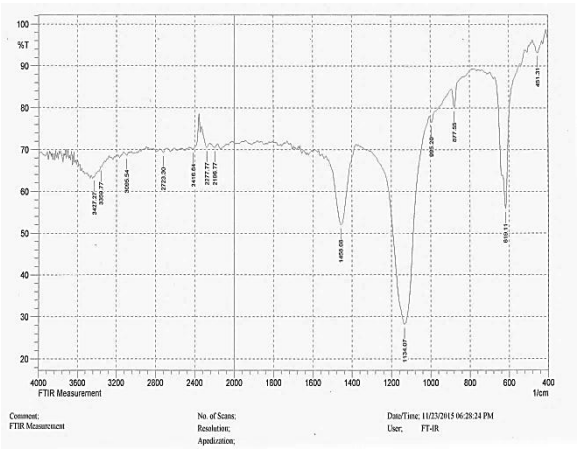

Fig. 1: FT-IR spectrum of compound

Thermal properties of a + b nanocomposites (DSC)

Based on experimented data executed by authors[12] ,nanocomposites a+b were investigated. As demonstrated (figure 3 and 4), the glass transition region exist over a temperature rang. Consequently, Tg located as the point of bending of the DSC curve at 82, 95 C° for (a and b) Composites Respectively. The melting temperature and expand of crystalling were observed to be constrained by the change in the filler surface modification, this ticked that underthe condition used for synthesis of the composites[13,] the modified filler had no impact on the crystallinity of the filler of nanocomposite (a)[14].The(DSC) thermogram of nanocomposite(b)exhibited a forward crystallization and a fibrous morphology rather than (Al PAN) or nanocomposite a, behavior.

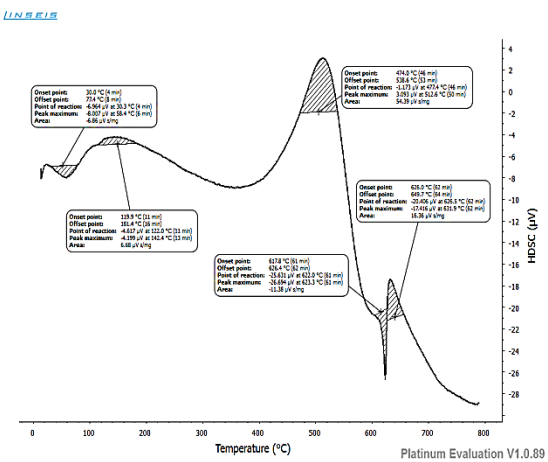

Fig. 3: DSC curve of compound(a)

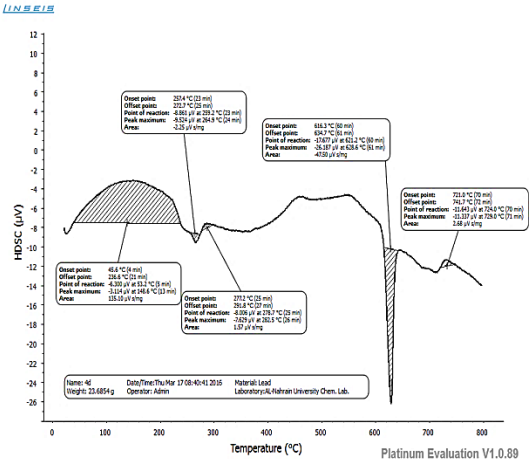

Fig. 4: DSC curve of compound(b)

Surface of Polymer – Metal oxide nanocomposite

The surface of the Al, polymer (a) and Pt, polymers (b), were spotted with atomic Microscope (AFM) fig (5and6). The image of AFM showed that the surface of the polymer brush was very soft because it contained polymer chins that had the same rise.

It is notion that the holes are created by oxygen evolution taking place during the oxidation process. Surface of the nano oxides layers were soft and did not show any divergence in height by more than 6 nm figures show the topographic structures in 2 D and 3D vision of AFM images of (a and b) nanocomposites layers builded on stainless steel specimen[15].

Avg. Diameter: 80.31 nm

Diameter(nm)<	Volume(%)	Cumulation(%)	Diameter(nm)<	Volume(%)	Cumulation(%)	Diameter(nm)<	Volume(%)	Cumulation(%)
40.00	1.44	1.44	70.00	10.07	31.65			
45.00	1.44	2.88	75.00	10.07	41.73	100.00	10.07	83.45
50.00	1.44	4.32	80.00	8.63	50.36	105.00	6.47	89.93
55.00	2.88	7.19	85.00	5.76	56.12	110.00	7.91	97.84
60.00	10.79	17.99	90.00	7.91	64.03	115.00	2.16	100.00
65.00	3.60	21.58	95.00	9.35	73.38			

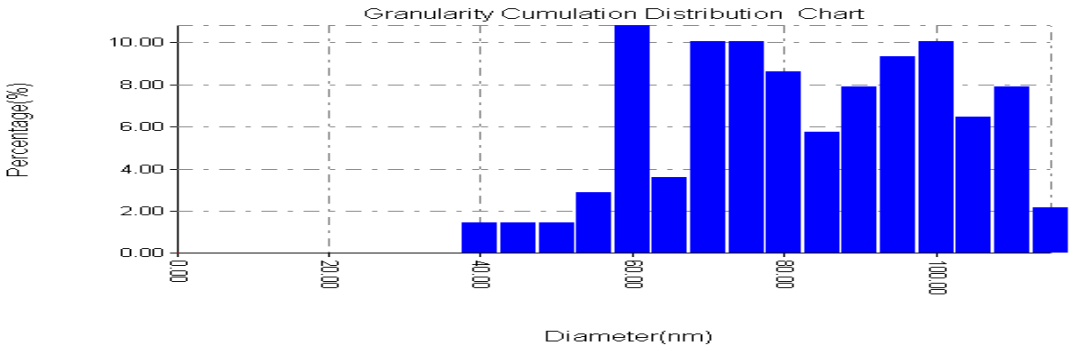

Fig. 5: The reprint of AFM reports for statistical measuring particle size and their distributions of nanometaloxides / polymer layers on SS 316 specimen (a)

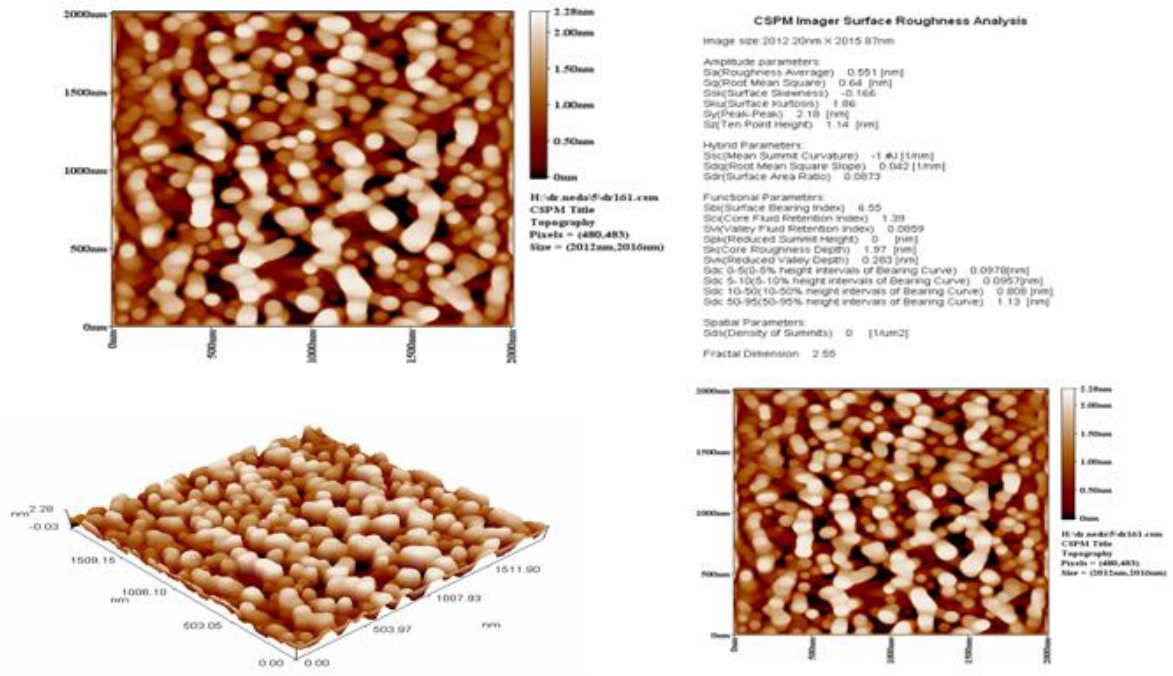

Fig. 6: in 2 D and 3D vision of AFM images of (a) nanocomposites layers builded on stainless steel specimen

Avg. Diameter:81.73 nm

Diameter(nm)<	Volume(%)	Cumulation(%)	Diameter(nm)<	Volume(%)	Cumulation(%)	Diameter(nm)<	Volume(%)	Cumulation(%)
70.00	10.77	10.77	90.00	10.77	78.46			
75.00	22.31	33.08	95.00	8.46	86.92	110.00	2.31	99.23
80.00	19.23	52.31	100.00	6.92	93.85	135.00	0.77	100.00
85.00	15.38	67.69	105.00	3.08	96.92			

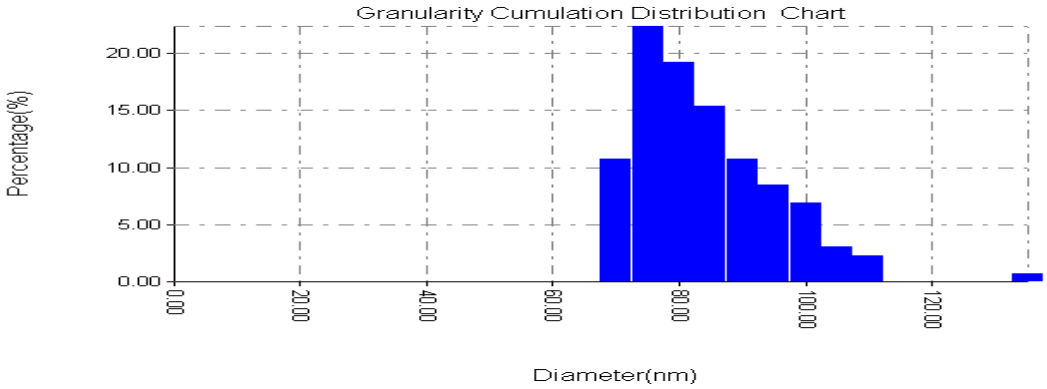

Fig. 7: the reprint of AFM reports for statistical measuring particle size and their distributions of nanometaloxides / polymer layers on SS 316 specimen (b)

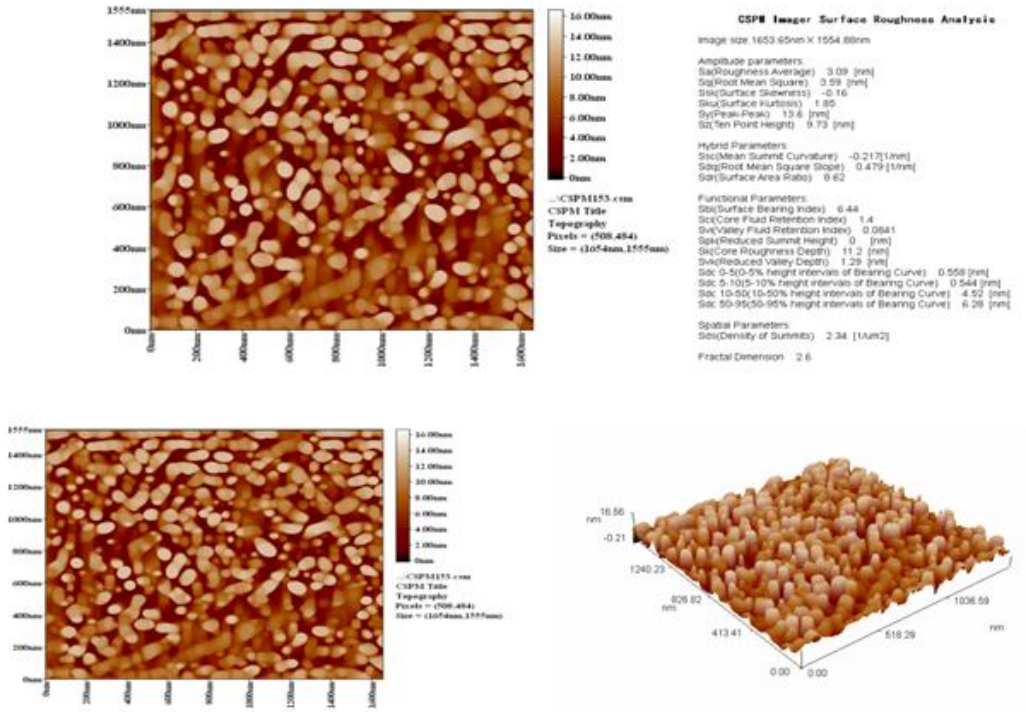

Fig. 8: in 2 D and 3D vision of AFM images of (b) nanocomposites layers builded on stainless steel specimen

X -ray diffraction pattern

The X -ray diffraction patterns of compounds a and b indications in figure (9and10) respectively, and are presented data of crystalline information several diffraction peaks in a (Al / PAN) patterns at 2θ =.12.0°, 28.0° ,31.7 ° and 45.6° were recorded, and peaks at 2θ =31.8 °,39.8°,46.3 ° and 67.5° were recorded in the XRD pattern of modified b (Pt / PAN), inclusion the presence of the order stricture of (a and b). It showed that these oxides crystallizes in a cubic crystal. The two oxides display spinal structures in the XRD patterns. Using (scherer's equation) in the table (2)[16].

Table 2: The unit cell dimensions of compounds at 500C°

Compounds	Particle size / AFM (nm) (avg.)	Crystal size nm
Al Fe_2O_4	80.31	38.076
Pt Fe_2O_4	81.73	36

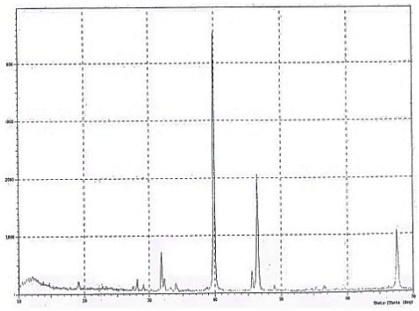

Fig. 9: XRD of compound (a)

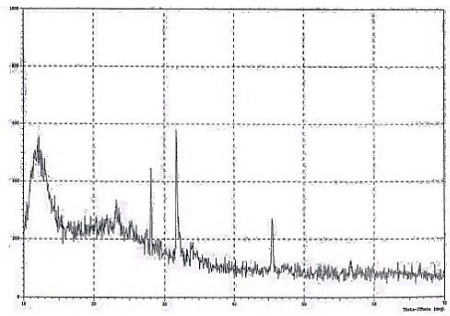

Fig. 10: XRD of compound(b)

Thermogravimetric analysis TG of DTG

Thermal analysis of (a and b) nanocomposites were presented in figures (11and12) respectively. Les 100 C° , the weight decreases result from moisture inside sample (water). The thermal behavior of the nanocomposites in TG of DTG thermaograms shows a coherence between the composite compounds and thermal degradation of the composites begins at a higher temperature (610-897 C°) referred to the high thermal decomposition of the composites[17] (table 3 and 4).

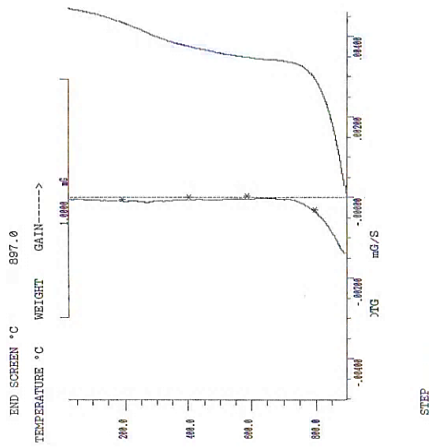

Fig. 11: TG and DTG curves of compound(b)

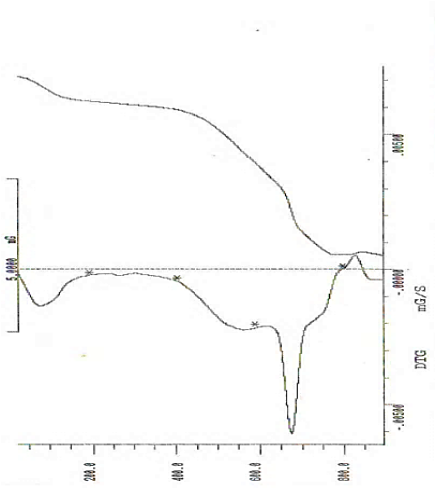

Fig. 12: TG and DTG curves of compound(a)

Tab 3: Thermal decomposition of the compound(b)

STEP		
START TEMP. °C		29.3
PEAK TEMP. °C		77.0
END TEMP. °C		306.7
δm	mG	-.91500
δm	%	-11.039
STEP		
START TEMP. °C		306.7
PEAK TEMP. °C		675.0
END TEMP. °C		787.7
δm	mG	-4.8920
δm	%	-59.018
RESIDUE		
TEMPERATURE °C		897.0
δm	mG	2.4670
δm	%	29.762

******** METTLER TA4000 SYSTEM *********

Tab 4: Thermal decomposition of the compound(a)

STEP		
START TEMP. °C		150.7
PEAK TEMP. °C		272.0
END TEMP. °C		298.0
δm	mG	-.07800
δm	%	-.80763
STEP		
START TEMP. °C		302.3
PEAK TEMP. °C		324.0
END TEMP. °C		350.0
δm	mG	-.02200
δm	%	-.22780
δm	mG	-.09000
δm	%	-.93187
STEP		
START TEMP. °C		740.0
PEAK TEMP. °C		896.0
END TEMP. °C		896.0
δm	mG	-.56800
δm	%	-5.8811
RESIDUE		
TEMPERATURE °C		897.0
δm	mG	8.8490
δm	%	91.624

******** METTLER TA4000 SYSTEM *********

Corrosion measurement estimation

Electrochemical corrosion kinetics of compounds (a and b) were characterized by main three polarization parameters involves, corrosion current density (I_{corr}), corrosion potential (E_{corr}) and tafel slopes, anodic region (βa) and cathodic region (βc),by a polarization curve($E_{vs.i}$) and the corrosion rate[18,19].The parameters accordions to the following eq. are given in table (5).

$$R_b = \frac{B}{i_{corr}} \text{ where}$$

$$B = \frac{B_a B_c}{2.303\ (B_{a+} B_c)}$$

$$\text{PE \%} = \left[1 - \frac{i_{corr}}{i^{\circ}_{corr}}\right] \text{ where PE\% is the inhibition efficiency}$$

i_{corr} and i°_{corr} are the corrosion current densities of uncoated and coated speciments respectively.
Al, Fe_2O_4 / PAN and Pt, Fe_2O_4 / PAN) / carbon steel in salin water (3.5% NaCl) system.

The potentiodynamic polarization curves of CS specimens under realization without and with nanocomposites a and b coating immersed in sea water at 293 k, are illustrate in figure (13 and 14) of uncoated and coated carbon steel for nanocomposites a and b respectively.The shift in Ecorr of the coated nanocaposites with comparison of the uncoated sample was display in table (5) corrosion measurements parameters for uncoated and coated carbon steel (CS) with nanocomposites specimens in 3.5% NaCl at 298k.

The results indicates the corrosion resistant advantage of the coating, as well it observed that the values of corrosion current density (icorr) for nano composites coated CS are lower than corresponding values for bare CS. The PE% of coated samples demonstrates the effect of coating process and the better protection ability for CS metal at 298k[20].

Table 5: Corrosion measurements parameters for coated and uncoated carbon steel (CS) with nanocomposites specimens in 3.5% NaCl at 298k

T(K)		E_{corr} (mV)	i_{corr} (μA/cm^2)	/Bc/ (mV/Dec)	/Ba/ (mV/Dec)	R_p Ω.cm^2	CR (gm/m^2.d)	CP (mm/y)	PE%	ρ%
Uncoated CS	293	-415.8	48.86	138.8	107.7	532.1	12.2	0.567	-	-
Coated CS with acrylonitrail + Al^{+3}	293	-242.3	6.22	129.0	117.4	4340.8	1.56	0.0722	87.3	0.30
coated CS with acrylonitrail + pt^{+4}	293	-367.1	4.31	126.6	118.5	6148.5	1.08	0.0501	91.1	3.1

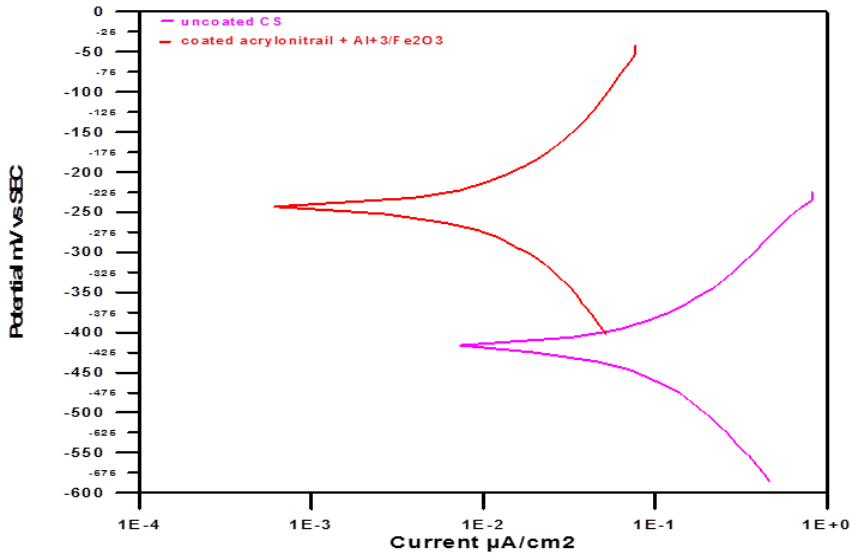

Fig. 13: Tafel plots of uncoated and coated *SS* 316 in 3.5NaCl of compound (a)

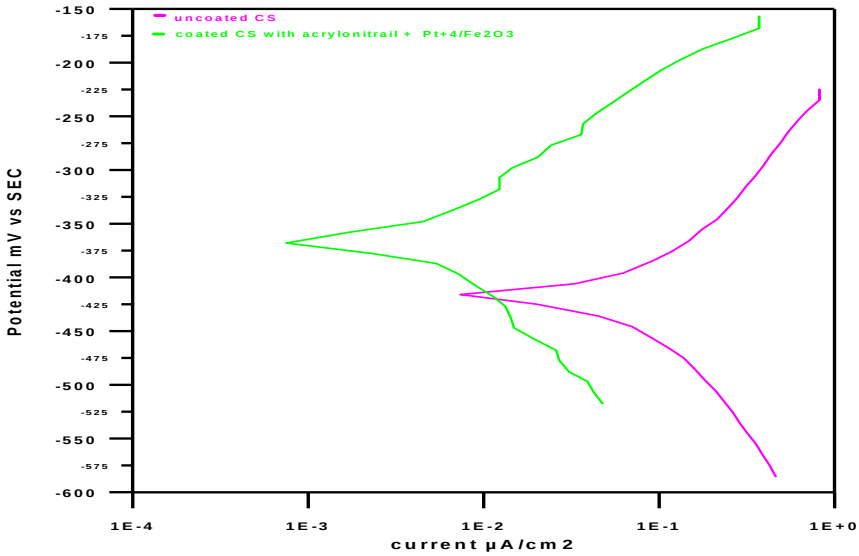

Fig. 14: Tafel plots of uncoated and coated *SS* 316 in 3.5NaCl of compound (b)

CONCLUSION

The nanocomposites were prepared by the reacts of ferric chloride, metal chlorides and acrylonitrile . FT-IR analysis displayed that the acrylonitrile polymerizes at low temperature and composes spinal ferrite. The study of XRD powder pattern and AFM images composes spinal crystal with crystalline size in the range of 36-38nm and with particle size of 80 -81nm. Both DSC and TG showed if there is presence of any excess of surface modification molecules existing as pseudo bilayer , but unbound to the polymers surface, the two nanocomposites (a and b) coated metals under investigation undergoes increasing of the corrosion protection properties at 293 k.

REFRENCES

1. Nam K, Tsutsumi Y and Yoshikawa C. Preparation of novel polymer- metal oxide nanocomposites with nanophase separal hierarchied structure. Bull Mater Sci. 2011;34(7): 1289-1296.
2. Vargo TG, Koloski TS and Macrae DM. Novel Nano- Metal polymeric composites Fabricated via In- situ self A ssembly, NSTI- Nanotech. 2006;2:772-777.
3. Vikas Mittal. Play Nanocomposites: Synthesis, Microstructure, and properties. Copyright c
4. Yu J, Lin RYF, poon B, Nazarenko S, Koloki TS, Vargo TG, Baer E and Hiltner A. Polymers with palladium Nano-particles as Active Membrane Materials. J Appl Polym Sci. 2004; 92.749.
5. Gubin SP, Koksharov YUA, Khomutov and YurkovG YU. Magnetic nanoparticles: preparation, structure and properties. Russian chemical Reviews. 2005;74:489-520.
6. Lau CMY. A stady of blending and complexation of poly(acrylic acid)/ poly (vinyl Ryrrolidone). Polymer. 2002;43(3):823-829.
7. Bashar Issa, Ihad M obaidat and Yousefhaik. Magnatic Nanoparticles :surface effect and properties Related to Biomedicine Applications. Int J Mol Sci. 2013;14(11):21266-21305.
8. Vargo TG, Koloski TS and Brupbacher JB. Novel Nano-metal polymeric composites Fabricated via In- situ self Assembly. www.nsti. Org, ISBN 0-9767985-7-3 vol.2,2006.
9. Tania Ribriro and Farinha T. Functional Functional Films from silica/ pohymen Nanoparticles". Materials. 2014;7:3881-3900.
10. Birendrap Singh, Jai P Singh, Jai P Singh and Shruti S. Synthesis and characterization of Inorganic polymer Nano- Composites. Der chemicasinica. 2012;3(2):521-526.
11. Sanchez C, Julian B and Belleville. Applications of hybrid organic-inorganic nanocomposites. J Mate Chem. 2005;15:3559–3592.
12. Jone M Barton. The application of differential scanning calorimetry (DSC) to the study of epoxy resinins curing reaction. 2004;27:111-154.
13. Vikas M. Polymer nanocomposites: sythesis, microstruture, and properties, copyright © wiley – VCH verlageGmb H & Co. KGaA, Weinheim ISBN: 978-3-527-32521-4, 2010.
14. Nam K, Tsutsumi Y, Tsutsumi Y, Yoshikawa C and others. Preparation of novel polymer – metal oxide nanocomposites with nanophase separated hierarchical structure. bull Mates Sa. 2011;34(7):1289-1296.
15. Oliveira M, Moraes J and Faez R. Impedance studies of poly (methyl methacrylate – co - acrylic acid) doped polyaniline on aluminum alloy. Progress in organic coatings. 65(3):348-356.
16. Yuan XY, Zou LL and Liao CC. Improved properties of chemically modified graphene / poly methyl methacrylate) nanocomposites via a facile in – situ bulk polymerization", express polymer letters. 2012;6(10):847–858.
17. Panl DR and Robeson LM. Polymer nanotechnology: nanocomposites. polymer. 2008;49:3187-3204.
18. Ale KsandraTurkovic. Metal oxide nano- particles and nano-composite polymer electrolytes – electrodes and electrolytes in solas and galvanic cells of the second generation", Actachimicaslovenica. 2008;55(4):822-827.
19. Bing Xue, YinshamJian and Darui Liu. Preparation and characterization of a Novel Anticorrosion Material", Materials Transations. 2011;52(1):96-101.
20. Uhliy HH and Revie RW. Uhlig's corrosion handbook. Val.51: John Wiley of sons, 2011.